AIP | Physics of Plasmas

Effect of cooler electrons on a compressive ion acoustic solitary wave in a warm ion plasma — Forbidden regions, double layers, and supersolitons

S. S. Ghosh and A. N. Sekar Iyengar

Citation: Physics of Plasmas (1994-present) **21**, 082104 (2014); doi: 10.1063/1.4891853
View online: http://dx.doi.org/10.1063/1.4891853
View Table of Contents: http://scitation.aip.org/content/aip/journal/pop/21/8?ver=pdfcov
Published by the AIP Publishing

Articles you may be interested in

Ion acoustic solitary waves and double layers in a plasma with two temperature electrons featuring Tsallis distribution
Phys. Plasmas **21**, 102901 (2014); 10.1063/1.4897177

Small amplitude dust ion-acoustic solitary waves and double layers in a dusty plasma with flat-topped electron distribution
Phys. Plasmas **17**, 123704 (2010); 10.1063/1.3526649

Effects of flat-topped ion distribution and dust temperature on small amplitude dust-acoustic solitary waves and double layers in dusty plasma
Phys. Plasmas **17**, 123706 (2010); 10.1063/1.3524562

Large amplitude dust acoustic solitary waves and double layers in positively charged warm dusty plasma with nonthermal electrons
Phys. Plasmas **17**, 014503 (2010); 10.1063/1.3291060

Dust acoustic solitary waves and double layers in a dusty plasma with two-temperature trapped ions
Phys. Plasmas **11**, 926 (2004); 10.1063/1.1643757

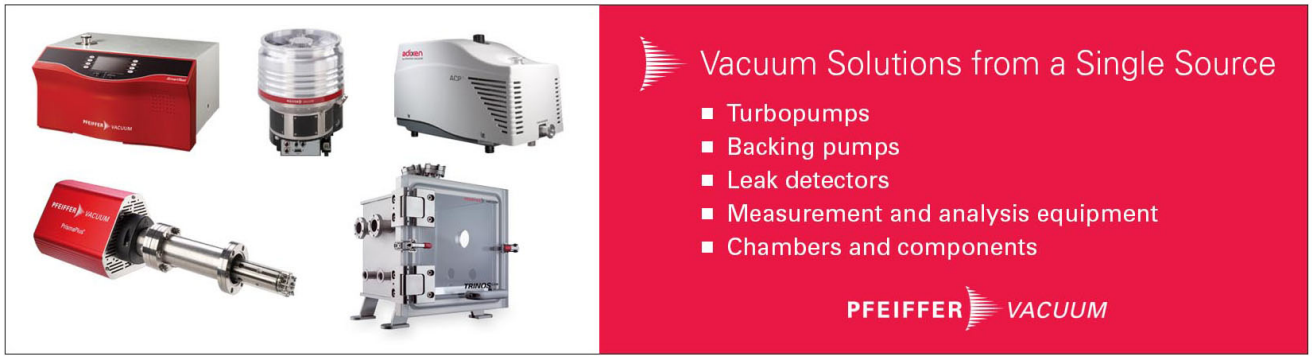

This article is copyrighted as indicated in the article. Reuse of AIP content is subject to the terms at: http://scitation.aip.org/termsconditions. Downloaded to IP: 14.139.123.135 On: Tue, 16 Dec 2014 06:25:22

PHYSICS OF PLASMAS **21**, 082104 (2014)

Effect of cooler electrons on a compressive ion acoustic solitary wave in a warm ion plasma — Forbidden regions, double layers, and supersolitons

S. S. Ghosh[1,a)] and A. N. Sekar Iyengar[2]
[1]*Indian Institute of Geomagnetism, New Panvel, Navi Mumbai 410218, India*
[2]*Plasma Physics Division, Saha Institute of Nuclear Physics, Kolkata 700064, India*

(Received 23 May 2014; accepted 21 July 2014; published online 4 August 2014)

It is observed that the presence of a minority component of cooler electrons in a three component plasma plays a deterministic role in the evolution of solitary waves, double layers, or the newly discovered structures called supersolitons. The inclusion of the cooler component of electrons in a single electron plasma produces sharp increase in nonlinearity in spite of a decrease in the overall energy of the system. The effect maximizes at certain critical value of the number density of the cooler component (typically 15%–20%) giving rise to a hump in the amplitude variation profile. For larger amplitudes, the hump leads to a forbidden region in the ambient cooler electron concentration which dissociates the overall existence domain of solitary wave solutions in two distinct parameter regime. It is observed that an inclusion of the cooler component of electrons as low as $< 1\%$ affects the plasma system significantly resulting in compressive double layers. The solution is further affected by the cold to hot electron temperature ratio. In an adequately hotter bulk plasma (i.e., moderately low cold to hot electron temperature ratio), the parameter domain of compressive double layers is bounded by a sharp discontinuity in the corresponding amplitude variation profile which may lead to supersolitons. © *2014 AIP Publishing LLC*.
[http://dx.doi.org/10.1063/1.4891853]

I. INTRODUCTION

Ion acoustic solitary waves (IASW) and weak double layers (WDLs) have been studied extensively for the last few decades theoretically,[1–8] experimentally,[9–15] and numerically.[16–23] Most of the early works were based on a weakly nonlinear analysis which truncates the higher order nonlinearity using the reductive perturbation method.[2] For an appropriate scaling,[24] the plasma system is governed by a class of integrable nonlinear partial differential equations (PDEs) which, when solved analytically with appropriate boundary conditions, give solitons. Apart from the celebrated Korteweg-de Vries (K-dV) equation,[25,26] solitons were also obtained by solving other nonlinear PDEs, like modified Korteweg-de Vries (mK-dV),[27] Kadomtsev-Petviashvilli (KP, for two dimensions),[28] Zakharov-Kujnetsov (ZK, for cylindrical geometry, applicable for magnetized plasma),[29] or nonlinear Schrödinger type equations (NLSE, for envelope solitons),[30] to name a few. Though have been studied by many authors,[26,27,29] they were, however, found to be inadequate to interpret large amplitude solutions, especially the electrostatic solitary wave (ESW) detected in the Earth's magnetosphere[31,32] as well as those observed in laboratory plasmas.[33] It was thus become evident that a weakly nonlinear analysis, which truncates the nonlinearity after the third, or some higher orders, needs to be complemented by a complete theory of arbitrary or large amplitude nonlinear waves.

Almost parallel to the reductive perturbation method, Sagdeev,[34] following the classical analogue of a particle in a potential well, developed a self-consistent analysis for an arbitrary amplitude wave by solving Poisson's equation as an energy integral in a co-moving wave frame. The method gained rapid popularity as it was found to be applicable for both fluid,[5,35,36] as well as kinetic models,[37–39] and used extensively for wide varieties of plasma systems.[5,40–43] The technique also enables one to understand the underlying physical processes by studying its respective profiles.[44] Recent growing interests in EPN (electron-positive ion-negative ion) plasma[15,45,46] and discovery of supersolitons[47–49] have rekindled the interest in the Sagdeev pseudopotential technique anew.

Of various multi-component plasma models studied by adopting Sagdeev pseudopotential technique, two electron temperature plasma gained particular interests as they are found to be ubiquitous in space and, particularly, in Earth's magnetosphere where cold electrons are of ionospheric origins and the hotter ones are impinged from the solar wind. Theoretically, because of their indistinguishable masses, coexistence of two distinct populations of electrons for a long time scale may sometimes become questionable.[50] The Cluster multi-spacecraft observations, however, confirmed the existence of both low and high temperature electron populations in the magnetospheric boundary layers.[51] The presence of two electron temperatures has also been reported in laboratory plasma where a secondary species of electrons appears due to the filament heating.[33] In the fluid limit, it is customary to assume electrons as massless where the

[a)]Electronic mail: sukti@iigs.iigm.res.in

 © 2014 AIP Publishing LLC

This article is copyrighted as indicated in the article. Reuse of AIP content is subject to the terms at: http://scitation.aip.org/termsconditions. Downloaded to IP: 14.139.123.135 On: Tue, 16 Dec 2014 06:25:22

frequency of the plasma wave (ion acoustic wave in this case) is far below than the corresponding electron plasma frequency. In the case of two distinct populations of electrons, it is then appropriate to assume that both the species are separately in thermal equilibrium, each one obeying Boltzmann distributions.[52] Jones *et al.*[53] was the first to study ion acoustic waves in the presence of two electron temperatures while Goswami and Buti[54] obtained the solitary wave solution for two electron temperatures in the presence of cold ions. It was soon become evident that the presence of a second electron species generates rarefactive (negative amplitude) solitary waves. The interrelation between rarefactive waves and WDLs were established by both theories[35] and satellite observations.[55] WDLs are particularly important as they play significant roles in particle accelerations in the auroral region. With the advance in satellite expeditions, there was an enhancement in the observational data which encouraged the study of the ion acoustic solitary wave in the presence of two electron temperatures.

In spite of the extensive theoretical analysis of ion acoustic rarefactive solitary waves for a two electron temperature plasma, the effect of the presence of the second electron species on a fully nonlinear compressive solution received comparatively lesser attentions.[56] The relative lacuna motivated us to delineate the entire parameter regime highlighting the effect of the second electron species on a compressive solitary wave solution. In this present paper, we have critically investigated the effect of the ambient density of the cooler component of electrons on the variation of the amplitude, width, density perturbations, and the existence domain of the compressive solitary wave. It was observed that the inclusion of a hotter species in a single ion plasma modifies the existing compressive solitary wave solution only marginally while inclusion of an extremely low concentration of cooler electrons in a relatively hotter plasma may bring drastic changes. The relative temperature and concentration ratios of the two electron components define the respective parameter regimes where the solutions exhibit distinctly different characteristics. Besides the usual solitary wave solutions, the presence of cooler electrons with a concentration as low as $\ll 1\%$ revealed compressive double layers followed by sudden changes of amplitudes and even supersolitons.[47] Pseudopotential profiles representing supersolitons are reported to comprise two subwells, leading to wiggles to the resultant electric field profile.[48,49] The analysis also reveals a preferred value of cooler electron concentration which yields maximum solitary wave amplitude for the system, leading to a forbidden region for the cooler electron concentration as the amplitude grows larger. Our findings are expected to be relevant for the studies in EPN plasmas,[15,45,46] where the negative ion plays the role of the cold electron providing a second negatively charged species.[57] Due to its large inertia, the presence of the negative ion affects the Debye shielding, thus modifying the solution significantly. We feel that, to understand such EPN plasmas, it is necessary to benchmark them with the study of an analogous system comprising two electron temperatures. The present study may also be applicable to ESWs observed in different boundary layers of Earth's magnetosphere.[58]

The paper is organized as follows. Sec. II presents the exact analytical form of the Sagdeev pseudopotential for a warm ion plasma containing two temperature electrons while Sec. III presents a critical analysis of the corresponding positive amplitude solution highlighting the effect of the second electron species. In Sec. III A, we have revealed an intermediate region in cooler electron concentrations which is devoid of any solitary wave solution (forbidden region). Section III B analyzes the effect of the electron temperature ratio on the forbidden region, while Sec. III C reveals the compressive double layer. The association of a compressive double layer with supersolitons has been studied in Sec. III D where we have delineated the overall existence domain highlighting the distinctly different characteristics of different parameter regimes. Section III E further shows the overall effect of Mach number and ion temperature on the double layer and Sec. IV presents the concluding remarks.

II. THE SAGDEEV PSEUDOPOTENTIAL

We have assumed a two electron temperature plasma where both the electron species are separately in thermal equilibrium obeying Boltzmann's distribution[59]

$$n_e = n_{ec} + n_{eh} = \mu e^{\frac{\phi}{\mu+\nu\beta}} + \nu e^{\frac{\beta\phi}{\mu+\nu\beta}}, \tag{1}$$

μ (ν) being the initial equilibrium densities for cold (hot) electrons and β ($= T_{ec}/T_{eh}$) is the cold to hot electron temperature ratio. Solving the basic set of the normalized fluid equations for warm adiabatic ions in an infinite, collision-less, unmagnetized plasma, we obtain the warm ion density[59]

$$n_i = \frac{1}{2\sqrt{3\sigma}}\left[\left\{\left(M+\sqrt{3\sigma}\right)^2 - 2\phi\right\}^{1/2} - \left\{\left(M-\sqrt{3\sigma}\right)^2 - 2\phi\right\}^{1/2}\right], \tag{2}$$

where σ ($=T_i/T_{eff}$) describes the finite ion temperature effect and the factor 3 occurs due to the specific heat ratio in an one dimensional system.[13] The subscripts i, e, c, and h refer to ion, total electron, and cold and hot electron components, respectively, and other notations have their usual meaning. All the number densities are normalized by the equilibrium plasma density n_0 (i.e., $\mu+\nu=1$), the time (t) and space (x) are normalized by the reciprocal ion plasma frequency ω_{pi}^{-1} ($\omega_{pi} = \sqrt{\frac{4\pi n_0 e^2}{m_i}}$) and effective Debye length λ_{eff} ($= \sqrt{\frac{T_{eff}}{4\pi n_0 e^2}}$) and the velocity ($v_i$) and the electrostatic potential (ϕ) are normalized by the effective ion acoustic speed c_{eff} ($= \sqrt{\frac{T_{eff}}{m_i}}$) and $\frac{T_{eff}}{e}$, respectively. The Mach number M is also normalized by c_{eff}. Putting Eqs. (1) and (2) in the Poisson's equation

$$\frac{\partial^2\phi}{\partial x^2} = n_{ec} + n_{eh} - n_i \tag{3}$$

and solving for the normalized boundary conditions, we obtain the familiar Sagdeev pseudopotential for a two electron temperature, warm ion plasma[44]

This article is copyrighted as indicated in the article. Reuse of AIP content is subject to the terms at: http://scitation.aip.org/termsconditions. Downloaded to IP: 14.139.123.135 On: Tue, 16 Dec 2014 06:25:22

$$\psi(\phi) = -\left[(\mu+\nu\beta)\left\{\mu\left(e^{\frac{\phi}{\mu+\nu\beta}}-1\right)+\frac{\nu}{\beta}\left(e^{\frac{\beta\phi}{\mu+\nu\beta}}-1\right)\right\}\right.$$
$$\left.+\frac{1}{6\sqrt{3\sigma}}\left\{\left[\left(M+\sqrt{3\sigma}\right)^2-2\phi\right]^{3/2}-\left(M+\sqrt{3\sigma}\right)^3-\left[\left(M-\sqrt{3\sigma}\right)^2-2\phi\right]^{3/2}+\left(M-\sqrt{3\sigma}\right)^3\right\}, \quad (4)$$

which satisfies the following energy equation:

$$\frac{1}{2}\left(\frac{d\phi}{d\eta}\right)^2+\psi(\phi)=0, \quad (5)$$

η $(=x-Mt)$ being the generalized coordinate for the corresponding steady state solution.

In order to have solitary wave solutions, this pseudopotential must satisfy following conditions:

$$\psi(0)=\frac{\partial\psi(0)}{\partial\phi}=0; \quad \frac{\partial^2\psi(0)}{\partial\phi^2}<0,$$
$$\psi(\phi_0)=0; \quad \frac{\partial\psi(\phi_0)}{\partial\phi}\neq 0 \quad \text{for} \quad \text{some}\ \phi_0,$$
$$\psi(\phi)<0 \quad \text{for} \quad 0<|\phi|<|\phi_0|, \quad (6)$$

where $|\phi_0|$ is the amplitude of the solitary wave. Equation (6) summarizes the boundary conditions determining the existence of solitary waves and ensures the recurrence of its initial state. For a double layer, however, both

$$\psi(\phi_0)=0 \quad \text{and} \quad \frac{\partial\psi(\phi_0)}{\partial\phi}=0, \quad (7)$$

needs to be satisfied which ensures the transition of the solution from one initial state to another final state.[60] A compressive (positive amplitude) solitary wave solution is further restricted by the energy condition

$$\phi_0<\frac{1}{2}\left(M-\sqrt{3\sigma}\right)^2 \quad (8)$$

beyond which the Sagdeev pseudopotential turns complex, indicating steepening and wave breaking owing to the reflection of ions from the potential hill.[3,44]

III. FULLY NONLINEAR SOLUTIONS

It is well known that solitary waves emerge due to the balance between nonlinearity and dispersion. Goswami and Buti[54] obtained the parameter

$$\Delta=\frac{\mu+\nu\beta^2}{(\mu+\nu\beta)^2}; \quad \Delta<3, \quad (9)$$

which determines the existence of the compressive solitary wave in a weakly nonlinear regime. The parameter was obtained from a K-dV equation governing the weakly nonlinear solution[26,54,61] and may be considered as a qualitative measurement of the extent of nonlinearity for any particular system. On the other hand, it has been observed that the effective temperature of electrons $T_{\rm eff}$ $[=T_{\rm ec}T_{\rm eh}/(\mu T_{\rm eh}+\nu T_{\rm ec})]$ may indicate the extent of dispersion.[56]

To understand the effect of the second electron species on a compressive solitary wave, we have plotted the variations of Δ (dashed lines) and $T_{\rm eff}$ (solid lines), respectively, with μ in Fig. 1 for different β values. It shows a monotonic increase in the dispersion ($T_{\rm eff}$, estimated in terms of $T_{\rm c}$) with decreasing μ, while the nonlinearity (Δ) shows a non-monotonic behaviour exhibiting humps at certain $\mu=\mu_{\rm c}$. Eventually, for a significantly low ambient cooler electron concentration ($\mu<\mu_{\rm c}$) and sufficiently large hot electron temperature (low β), it shows a sharp increase in the dispersion ($T_{\rm eff}$) in contrast with the decrease in the nonlinearity for a decreasing μ, suggesting a possible non existence of compressive solitary waves below certain minimum value of μ, whereas for a larger β (i.e., $\beta\to 1$), both the nonlinearity and the dispersion remain comparable throughout the range.

A. Forbidden regions

To ascertain our conjecture as mentioned above (i.e., in Fig. 1), we have delineated the parameter regime for varying ambient cooler electron concentrations. The electron temperature ratio has been chosen to be large enough to ensure a compressive solitary wave solution ($\beta=1/5$). Compared to the electron parameters, the effect of the ion temperature remains marginal. Hence, σ $(=1/30)$ has been assumed to be constant throughout our study.

Figure 2 shows the variation of the solitary wave amplitude with μ for different Mach numbers (M) while $\beta=1/5$ remains constant. It, too, shows a non-monotonic behavior which resembles the variation of Δ (the nonlinearity) in

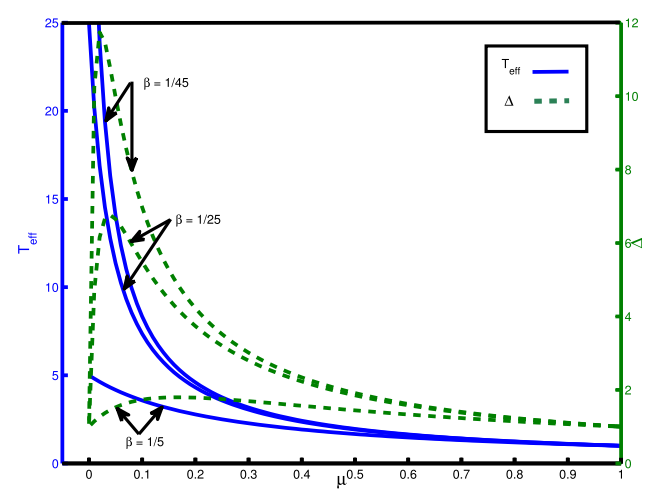

FIG. 1. Variation of nonlinearity (Δ) and dispersion ($T_{\rm eff}$) with μ for different β.

This article is copyrighted as indicated in the article. Reuse of AIP content is subject to the terms at: http://scitation.aip.org/termsconditions. Downloaded to IP: 14.139.123.135 On: Tue, 16 Dec 2014 06:25:22

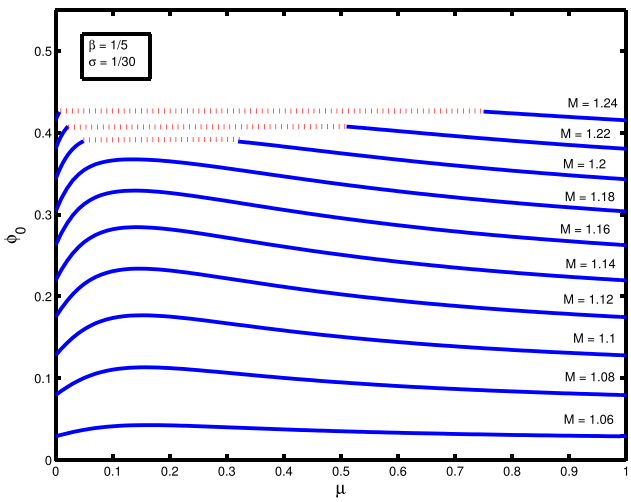

FIG. 2. Variation of amplitude with μ for different M ($\beta = 1/5$). Dotted lines denote the "forbidden regions" in μ.

Fig. 1. Initially, inclusion of a cooler species increases the amplitude, but beyond certain critical value (e.g., $\mu = \mu_c$), the amplitude starts decreasing with increasing μ giving rise to a hump at certain μ_c. As expected, the amplitude increases with increasing M. For further increase in M (e.g., $M > 1.18$), the hump disappears giving rise to a "forbidden region" in μ. For some minimum value of μ ($\mu = \mu_{\min}$, $\mu_{\min} > \mu_c$), the solution terminates due to the energy principle (Eq. (8)), but reappears for a sufficiently lower value of μ ($\mu < \mu_c$) restoring the single electron solution at $\mu = 0$ which is qualitatively equivalent to $\mu = 1$ (i.e., single electron) state.

It is particularly interesting to note the hump-like (non monotonic) variation as it may indicate two competitive processes in the plasma. Inclusion of a cooler component of electrons increases nonlinear effects (Δ) and the amplitude increases. On the other hand, inclusion of a hotter component increases the effective energy of the system (T_{eff}) which also leads to an increase in the amplitude. For major part of this variation, the solution is governed by the effective energy of the system ($\mu > \mu_c$), while for a sufficiently low μ ($\mu < \mu_c$), the effect of nonlinearity due to the presence of a second electron species dominates. This also shows that the effect of the second electron species mainly arises due to the presence of a minority component of cooler electrons, whereas the inclusion of a minority component of the hotter species deviates the solution only marginally from that for a single electron plasma.

We have estimated the maxima of the Δ variation curves in Fig. 1 analytically by differentiating Eq. (9) with μ

$$\mu^* = \frac{\beta}{1+\beta}, \tag{10}$$

where μ^* ($\approx\beta$) is the estimated maxima which depends solely on β. We have also estimated μ_c, the critical value of μ corresponding to the largest amplitude for any particular M - β regime, numerically from Fig. 2. In Fig. 3, we have plotted the variations of both μ_c (solid lines) and μ^* (dashed line) with β for different M, where the latter denotes the corresponding weakly nonlinear limit. It shows that both μ_c and μ^* decrease with decreasing β (increasing hot electron temperature), while the increase in M further tends to lower the value of μ_c, indicating a possible shift of the maxima (the hump in Fig. 2) to a lower μ. The M dependence of the maxima appears to be the consequence of the higher order nonlinearity whereas at the weakly nonlinear limit, it turns to be independent of M (Eq. (10)). The value of μ^* further determines the upper bound of μ_c (i.e., $\mu^* > \mu_c$) throughout the region whereas for a weakly nonlinear, or small amplitude limit (i.e., low M – large β solutions), the μ_c variation merges asymptotically with that for μ^* ($\mu_c \to \mu^*$), the latter being solely determined by the corresponding β value.

Figures 1–3 reveal significant effects of the cooler electron component on the compressive ion acoustic solitary waves. To compare the relative roles played by the two different electron species, we have plotted the relative density perturbations of cold (hot) electrons, viz., $\delta n_c^* (\delta n_h^*)$, represented by dashed-dotted (dashed) lines, respectively, and the overall charge separation, Δn, represented by the solid line, in Fig. 4. We have chosen a single Mach number, viz., $M = 1.1$. The different parameters are defined as

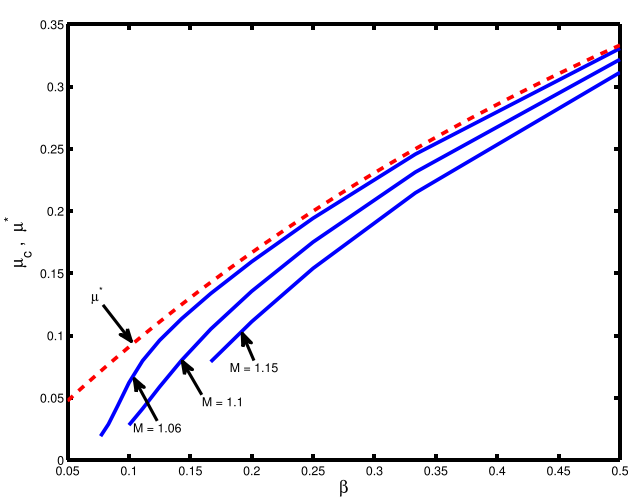

FIG. 3. Variation of μ_c (solid lines) and μ^* (dashed line) with β for different M.

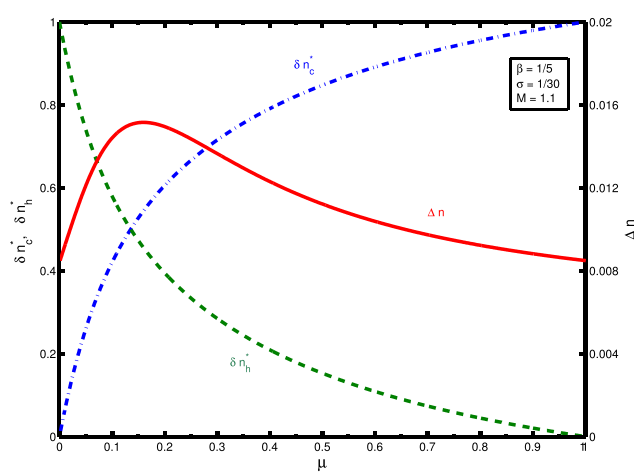

FIG. 4. Variation of relative density perturbations δn_c^* (dotted line), δn_h^* (dashed line), and the total charge separation Δn (solid line) with μ for $M = 1.1$ and $\beta = 1/5$.

This article is copyrighted as indicated in the article. Reuse of AIP content is subject to the terms at: http://scitation.aip.org/termsconditions. Downloaded to IP: 14.139.123.135 On: Tue, 16 Dec 2014 06:25:22

$$\delta n^*_{\mathrm{c,h}} = \frac{\delta n_{\mathrm{c,h}}(\phi_0)}{\delta n_{\mathrm{e}}(\phi_0)}; \quad \Delta n = n_{\mathrm{i}}(\phi_0) - n_{\mathrm{e}}(\phi_0), \tag{11}$$

where $\delta n_{\mathrm{j}}(\phi_0)$ is the density perturbation at the maximum amplitude ϕ_0 for the j-th component, j $(=c, h, e)$ being the cold, hot, and the total electron species, respectively. The figure shows that the contribution of the cold electrons in total electron density perturbation increases with initial ambient cold electron density (μ) while that for the hot electron decreases. For $\mu \approx \mu_{\mathrm{c}}$, the contributions of both the cold and the hot electrons in overall electron density perturbation becomes equal ($\approx$50%) which maximizes the effect of the presence of two electron temperature species, as well as the overall charge separation (Δn), and leads to the maximum possible amplitude for the chosen Mach number. In other words, the condition for the critical value of μ (i.e., μ_{c}) can be readily obtained graphically by equating the relative contributions of the cooler and hotter species to the overall electron density perturbations, viz.,

$$\delta n^*_{\mathrm{c}} = \delta n^*_{\mathrm{h}}. \tag{12}$$

The analysis supports our aforementioned discussion on the effect of the second electron species for the case where the cooler component is the minority one. This also suggests that an optimum 15%–20% of initial cooler electron concentration provides the largest amplitude for the compressive solitary wave, and it decreases steadily for both the sides.

A similar hump-like variation could be noted in Baboolal *et al.*[35] for cold ions, though there was no further comment on it. Murthy *et al.*[61] reported forbidden regions in μ for weakly nonlinear solutions which arose due to the violation of the condition described by Eq. (9). In the present case of fully nonlinear solutions, however, the forbidden regions appear due to the competitive processes which arise due to the inclusion of the second electron species. A comparison between Figs. 1 and 2 reveals that, for a large Mach number ($M > 1{,}18$), both the nonlinearity and the effective energy of the system increase with the decreasing μ, leading to a sharp increase in the amplitude, followed by steepening

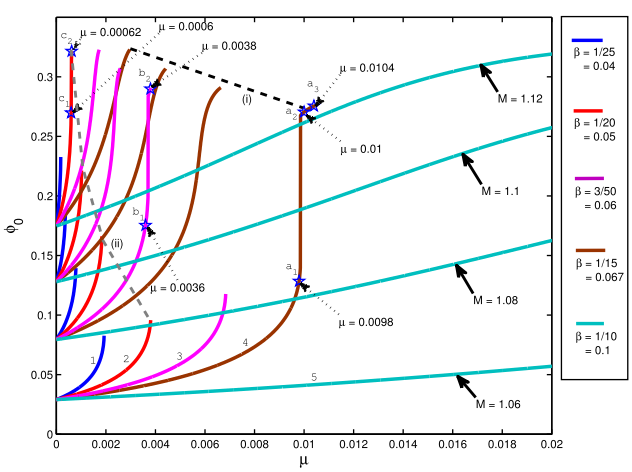

FIG. 5. Variation of amplitude with μ for the low μ regime ($\mu \leq 0.02$). Points $a_{1,2,3}$, $b_{1,2}$, and $c_{1,2}$ denote specific values of (ϕ_0, μ) and the dashed lines (curves (i) and (ii)) represent the variation of μ_{x} with M. Each set of curves belongs to a specific M ($=1.06-1.12$) while curves 1–5 denote different β.

and wave breaking. The solution terminates due to the violation of energy principle (Eq. (8)) resulting to a forbidden region beyond some $\mu_{\min}$ ($\mu_{\min} > \mu_{\mathrm{c}}$). For a sufficiently low μ and moderately hot electrons (large β), it reappears due to the decrease in nonlinearity. The solution in this regime is dominated by the variation of nonlinearity, rather than the effective energy of the system. The plasma is, eventually, dominated by the minority component of cooler electrons and the effect turns maximum when the contributions of both the species become equal (Fig. 4 and Eq. (12)).

B. Effect of β

The dependence of μ_{c} on β in Fig. 3 indicates that the appearance and extent of the forbidden region may substantially depend on the corresponding β value. In Fig. 5, we have delineated the low μ regime ($\mu \ll \mu_{\mathrm{c}}$) by plotting the variation of the amplitude with μ for different β and M. As expected, for $\mu = 0$, the effect of β vanishes and all the curves converge to the corresponding single-electron amplitude. With an inclusion of very low concentration of cooler electrons, the curves diverge, highlighting the effect of the electron temperature on the variation profile. Interestingly, it shows two distinctly different variation profiles depending on the range of β. For a low β regime (e.g., $\beta < 1/10$), there is a sharp increase in the amplitude with increasing μ. The variation profile appears to be "concave," i.e., its slope increases with increasing μ ($d^2\phi_0/d\mu^2 > 0$). On the other hand, for a larger β ($\beta = 1/10$) and low M ($M = 1.06$), the initial variation appears to be almost "linear" exhibiting slow increase in the amplitude with increasing μ. As M increases (viz., $M = 1.12$), the variation profile actually turns "convex," i.e., its slope decreases with μ ($d^2\phi_0/d\mu^2 < 0$). This indicates that the low μ regime is further comprised of two distinctly different regions characterized by low and large β values, respectively.

We have further noticed that, for $M = 1.06$ and an intermediate β (viz., $\beta = 1/15$), the variation profile shows a sharp discontinuity, or "jump condition," between points a_1 ($\phi_0 = 0.1284$, $\mu = 0.0098$) and a_2 ($\phi_0 = 0.2705$, $\mu = 0.01$) in Fig. 5 where a very small increase in the initial cooler electron concentration (0.02%) leads to a 110% increase in the amplitude. The solution terminates at a_3 ($\phi_0 = 0.2755$, $\mu = 0.0104$) where a further increase in μ causes only a marginal increase (1.8%) in the amplitude. As M increases (viz., $M = 1.08$), the variation curve for the particular β value ($\beta = 1/15 = 0.067$) smoothens, though a similar "jump condition" now shifts to a lower β (i.e., points b_1–b_2, $\beta = 0.06$) and the trend continues (e.g., points c_1–c_2, $M = 1.12$, $\beta = 0.05$). The unexpected sharp discontinuity observed in Fig. 5 appears to be fairly regular rather than accidental and reveals some possible transition processes triggered by the variation of β.

The two dashed lines in Fig. 5, viz., curves (i) and (ii), further show the variation of μ_{x} with M for two different β (viz., $\beta = 1/15$ and 1/20) where μ_{x} is the maximum value of μ beyond which the solitary wave solution terminates for the low μ regime (i.e., $\mu_{\mathrm{x}} \ll \mu_{\mathrm{c}}$). It shows that μ_{x} increases with decreasing M. The variation is approximately linear (curve

This article is copyrighted as indicated in the article. Reuse of AIP content is subject to the terms at: http://scitation.aip.org/termsconditions. Downloaded to IP: 14.139.123.135 On: Tue, 16 Dec 2014 06:25:22

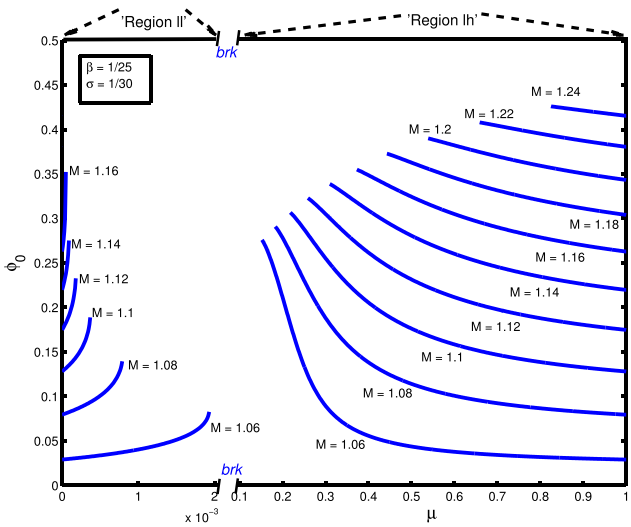

FIG. 6. Variation of amplitude with μ for different M ($\beta = 1/25$); "*brk*" denotes the "break" in the scale.

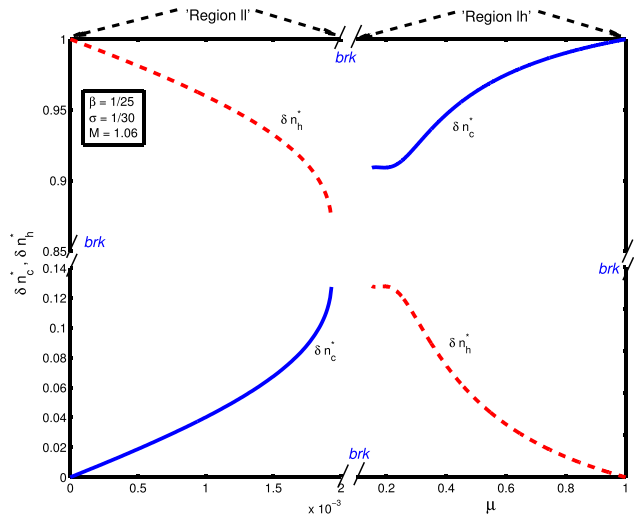

FIG. 7. Variation of relative density perturbations δn_c^* (solid line) and δn_h^* (dashed line) with μ for $M = 1.06$ and $\beta = 1/25$; "*brk*" denotes the "break" in the scale.

(i)) for a larger β ($= 1/15$), whereas for a lower β ($= 1/20$), the variation is much sharper (curve (ii)). For all M values, μ_x remains significantly smaller for a lower β.

C. Compressive double layers

Noting that the hot to cold electron temperature ratio (β) may play a pivotal role in determining the characteristics of the solution (Fig. 5), we have revisited our analysis in Sec. III A for a low β value ($\beta = 1/25$). Figure 6 shows the variation of the amplitude with μ for different M, keeping β ($= 1/25$) a constant. Inclusion of a hot electron component (decrease in μ) increases the amplitude and the variation pattern remains the same as Fig. 2 for up to $\mu \geq 0.5$. Beyond that value (i.e., $\mu \leq 0.4$), the amplitude increases sharply and the solution terminates for some $\mu_{\min}$ following the energy relation (Eq. (8)), where $\mu_{\min}$ depends on the Mach number and increases with increasing M. Apparently, there was no forbidden region or reappearance of solitary waves for lower μ value. The variation pattern appeared to be monotonic and bounded by $\mu \geq 0.2$ (the r.h.s. of Fig. 6).

To restore the solutions in the low μ regime, we have changed the scale and shown it with a "break in the scale" in the l.h.s. of Fig. 6. We found that the region at the lower μ is bounded by $\mu \leq 0.002$. The concave shaped variation profiles, as observed in Fig. 5 (Sec. III B), reappear confirming the existence of forbidden regions which are now bounded by the upper and lower limits of μ, viz., $0.002 < \mu < 0.2$ for $M = 1.06$, and its extent increases with M. The variation profiles remained characteristically different from those obtained for a large β solution (Fig. 2), as well as from those observed for a larger μ value (i.e., r.h.s. of Fig. 6). Consequently, it reveals two mutually exclusive existence domains for solitary wave solutions, viz., "region lh" for $\mu > 0.2$ (i.e., "low β – high μ" regime), and "region ll" for $\mu < 0.002$ (i.e., low β – low μ regime), respectively. For the latter ("region ll"), the amplitude increases smoothly with increasing μ and the solution terminates at much lower amplitude, without violating the energy relation (Eq. (8)). This also reveals a wide disparity in amplitudes at the two ends of the forbidden region. Unlike a large β solution (Fig. 2), where amplitudes at the both ends remain comparable, in the present case the left-end ("region ll") shows a much smaller amplitude compared to the right ("region lh"). This also confirms that, unlike other parameter regime, solitary wave solutions in "region ll" do not terminate due to wave steepening and breaking. Recalling that the region ("region ll") is expected to have large dispersion (Fig. 1), the waves may get "stretched" and "damped" causing the disappearance of the solution at much lower amplitude.

Following Sec. III A, we have plotted the variation of relative density perturbations for the cold (solid line) and hot (dashed lines) electrons in Fig. 7, keeping M ($= 1.06$) a constant. This shows that "region lh" is governed by the cold electron dynamics, while "region ll" is governed by the hotter one. At both sides, the solution disappears much prior to the region where the condition Eq. (12) may hold. For "region lh," the contributions turn to saturate prior to their

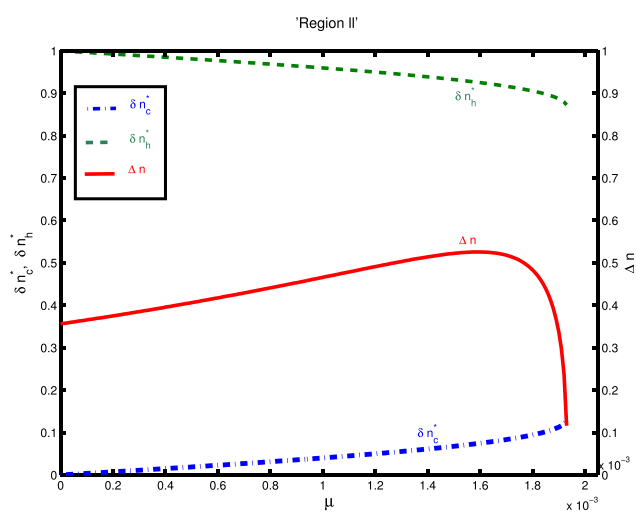

FIG. 8. Variation of relative density perturbations δn_c^* (dashed-dotted line), δn_h^* (dashed line), and charge separation Δn (solid line) with μ for "region ll"; $M = 1.06$ and $\beta = 1/25$.

This article is copyrighted as indicated in the article. Reuse of AIP content is subject to the terms at: http://scitation.aip.org/termsconditions. Downloaded to IP: 14.139.123.135 On: Tue, 16 Dec 2014 06:25:22

terminations, while in "region ll" they vary monotonically. Interestingly, in "region ll," an initial concentration of cooler electrons as low as less than 0.2% ($\mu < 0.002$) contributes more than 12% of the total electron density perturbations at the vicinity of the maximum amplitude ϕ_0 (Fig. 7) which may indicate a significant confinement of the cooler species within the perturbed region.

To highlight the "region ll," we have plotted the relative density perturbations, viz., δn_c^* (dashed-dotted line), δn_h^* (dashed line), and the charge separation Δn (solid line) for "region ll" in Fig. 8. It shows a sharp decrease in the charge separation (Δn) prior to the termination of the solution. This contradicts our analysis in Sec. III A (Fig. 4) where Δn increases monotonically with μ for $\mu < \mu_c$, i.e., prior to the forbidden region. This also contradicts our previous findings where we have observed an increase in the charge separation near the vicinity of the forbidden regions in the ion temperature.[44] On the other hand, Eq. (7) for double layers suggests a collapse in the charge separation. This further confirms that the compressive solitary wave solutions in "region ll" are distinctly different from those of other parameter regime.

To characterize the solutions observed in "region ll," we have plotted the variation of the width with μ (solid line) vis-à-vis that of the amplitude (dashed line) for both "region ll" and "region lh" in Fig. 9. In "region lh," the width increases with decreasing amplitude which is consistent with a K-dV or K-dV like soliton. Initially, the width shows a sharp increase which gradually tends to saturate with increasing μ, confirming an exactly opposite trend vis-à-vis that of the amplitude. In "region ll," on the other hand, both the amplitude and the width increase with increasing μ. Particularly, there is a sharp increase in the width as the solution approaches to the forbidden region (i.e., $\mu \to \mu_x$). This indicates that, in spite of being a small amplitude one, the solitary waves obtained in "region ll" are different from the usual weakly nonlinear (i.e., K-dV like) solutions.

For large amplitude rarefactive (i.e., negative amplitude) solitary wave solutions, the width-amplitude variation profiles are known to show anomalous width variations where, unlike K-dV solitons, the width increases with the increasing amplitude but for smaller amplitudes, they restore the usual K-dV like relation showing a decrease in the width with increasing amplitude.[59,60] Compressive solitary waves, being of smaller amplitudes compared to their rarefactive counterpart, have so far consistently showed a K-dV like variation. The "anomalous width variation" observed in "region ll" is thus the first report of its kind where it has been found to be associated with a compressive solitary wave. The result is particularly more surprising because, so far, anomalous width variations have been attributed to be a large amplitude phenomena while the amplitude of the solitary waves in this case is considerably small ($\phi_0 < 0.1$). In fact, the (normalized) amplitude is even smaller than that of a regular region ("region lh") which shows a K-dV type behaviour. This also contradicts the idea that the anomalous width variation is the characteristics of rarefactive solutions only. Interpretation of such behaviour thus poses serious questions and needs to be investigated in more detail.

We have previously observed that, for a rarefactive solitary wave, an anomalous width variation is followed by a double layer solution.[60] Figures 7 and 8 further suggest the possibility of a double layer solution in "region ll." In Fig. 10, we have plotted the corresponding Sagdeev pseudopotentials for different μ values, keeping $M = 1.06$ a constant. It confirms a double layer solution for $\mu = 1.9325 \times 10^{-3}$ with an amplitude $\phi_{dl} \approx 0.875$, where ϕ_{dl} is the double layer amplitude. The particular Sagdeev pseudopotential satisfies the condition of Eq. (7) ensuring its transition to another state (Sec. II). As M increases (i.e., $M > 1.1$), the solution disappears. Figure 5 suggests that, for increasing M, the region may be pushed to a much lower value of μ which may not be physically sustainable.

Ion acoustic double layers have been studied by many authors.[59,62–67] While the rarefactive (negative amplitude) double layers are well known for decades,[68,69] its compressive (positive amplitude) counterpart is comparatively lesser known. In other words, double layers are generally expected to be associated with a negative amplitude (rarefactive) solution rather than a positive one.[70,71] Goswami and

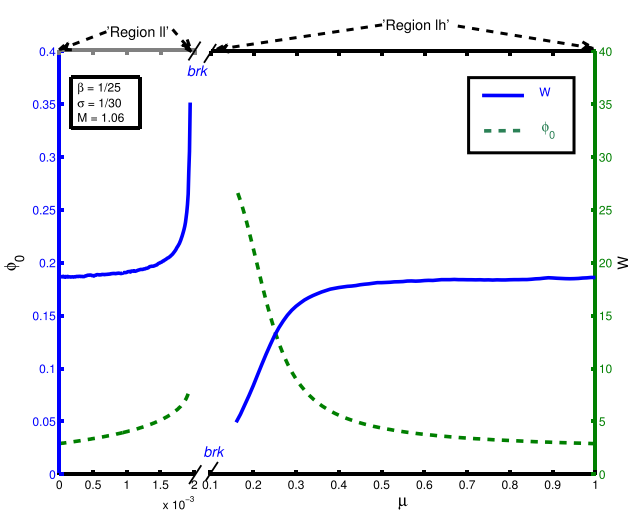

FIG. 9. Variation of width W (solid line) and amplitude ϕ_0 (dashed line) with μ for $M = 1.06$ and $\beta = 1/25$; "*brk*" denotes the "break" in the scale.

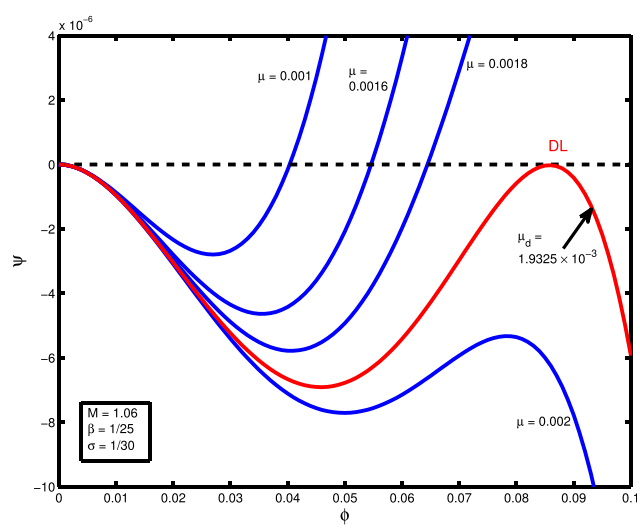

FIG. 10. Sagdeev pseudopotentials for the "low μ – low β" regime ("region ll") for different μ; $\mu < 0.002$. "DL" denotes the compressive double layer.

This article is copyrighted as indicated in the article. Reuse of AIP content is subject to the terms at: http://scitation.aip.org/termsconditions. Downloaded to IP: 14.139.123.135 On: Tue, 16 Dec 2014 06:25:22

Bujarbarua[72] were one of the first who reported compressive double layers in an EPN plasma. Compressive double layers in the presence of negative ions have also been observed by others for both weakly nonlinear[46,73] as well as general, large amplitude solutions.[57] It was observed that the existence and characteristics of such double layers depend on the density and temperature of the negative ion[73] and on its mass as well.[46] The role of the negative ion in these cases seems to be analogous to that of the second electron species while for the former one it is further modified due to its inertia.[57] Compressive ion acoustic double layers have also been reported in an e-p-i plasma,[74–76] dust ion acoustic waves,[77] as well as in an e-p-i plasma in the presence of negatively charged dust.[78] For an usual e-i plasma, however, compressive ion acoustic double layers appear to be less feasible[70] or marginal.[79] We have previously obtained compressive ion acoustic double layers for a two electron temperature, warm ion plasma[80] while Verheest *et al*.[81] reported the same in the presence of two positive ions and single electron species. Both the results ascertain that, like a rarefactive one, it is essential to have a three component plasma for the formation of a compressive double layer.

D. Supersolitons

Our analysis presented in Secs. III A–III C suggests two distinct phases of compressive solitary wave solutions. For the major part of the parameter regime, the solitary wave terminates due to the violation of the energy relation (Eq. (8)). As the amplitude reaches the limit ($=\frac{1}{2}M^2$), the ions start getting reflected from the potential hill,[44] leading to a wave breaking. The existence domain is thus determined by the relative balance between the K.E. ($\approx\frac{1}{2}M^2$) and the P.E. ($\approx\phi_0$) of the ions. There, however, exists a relatively small but distinct phase of solutions where a very minute proportion of cooler electrons are introduced in a hotter plasma. They get largely confined within the perturbed region, thus possibly disrupting the symmetry of the structure which leads to a compressive double layer terminating the corresponding solitary wave solution. This region also shows an anomalous increase in the width with increasing amplitude. Figure 5 further suggests a sharp transition between these two phases (Sec. III B).

To ascertain our findings and noting the distinct role played by the respective electron temperatures, we have plotted the variation of μ_x, as obtained numerically from Fig. 5, in Fig. 11(a) (upper panel) for a range of β values. To cover a wide range of variations, we have kept $M=1.06$. In the absence of any forbidden region, μ_x has been taken to be 1. It clearly shows two distinct regions, viz., "*A*" (no forbidden region) and "*B*" (forbidden region), respectively, while β_f ($=0.0782$) is the lowest value of β ensuring no forbidden region. The variation of μ_x for the forbidden region (i.e., region B), has been further highlighted by the dotted line with its scale shown at the r.h.s. ($\mu_x \leq 0.04$). It shows that, as β decreases μ_x is pushed to a lower value which is consistent with Fig. 5. We have chosen β_n ($=0.0192$) as our lowest limit of β (i.e., $\beta_n \leq \beta \leq 1$) for which μ_x reduces to 0.0002. A further decrease in β would reduce μ_x further which has been discarded as non-physical.

In Fig. 11(b) (middle panel), we have plotted the solitary wave amplitude ϕ_x corresponding to $\mu=\mu_x$. It readily reveals two sub-regions "*B*1" and "*B*2" within "*B*" of the upper panel, marked by β_c ($=0.065$), a critical value of β, below which the amplitude drops abruptly. Unlike the discontinuity observed at β_f (i.e., between "*A*" and "*B*1"), where μ changes from 1 (single electron) to ≈ 0.04 (two electron), the present one occurs in spite of a smooth variation of μ at β_c (upper panel). This emphasizes that the "jump condition" observed in Fig. 5 is a regular transitional effect rather than a possible singular artifact. Compared to "*B*2" (i.e., $\beta<\beta_c$), where the amplitude decreases smoothly and monotonically

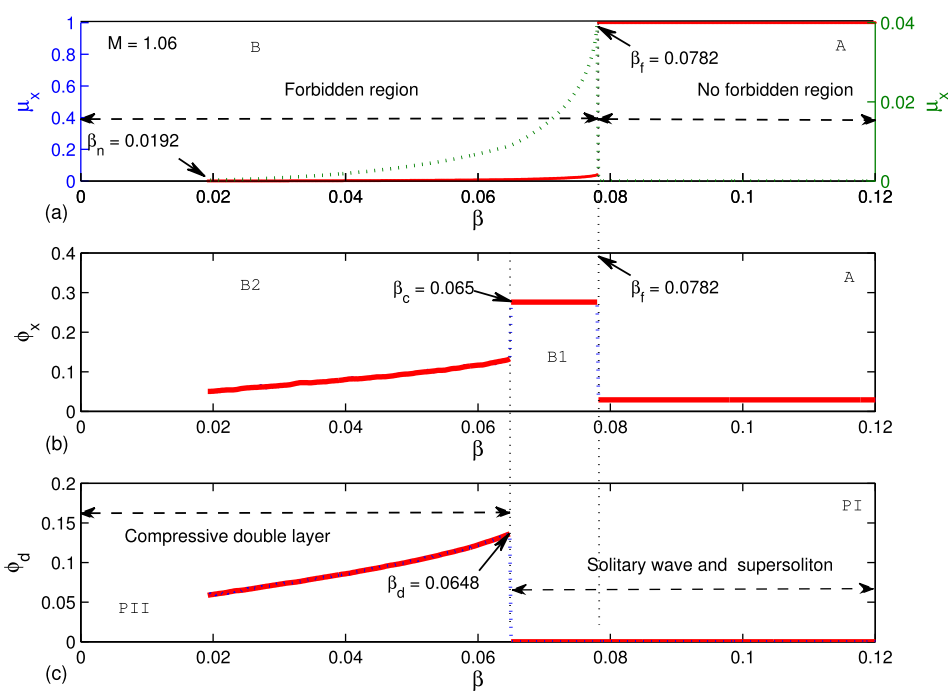

FIG. 11. Variation of (a) μ_x, the maximum μ for the solitary wave solution in low μ regime ($\mu_x \ll \mu_c$), (b) ϕ_x, the amplitude of the solitary wave at μ_x, and (c) ϕ_d, the corresponding double layer amplitude, with β; $M=1.06$. The vertical dotted lines mark different regions.

This article is copyrighted as indicated in the article. Reuse of AIP content is subject to the terms at: http://scitation.aip.org/termsconditions. Downloaded to IP: 14.139.123.135 On: Tue, 16 Dec 2014 06:25:22

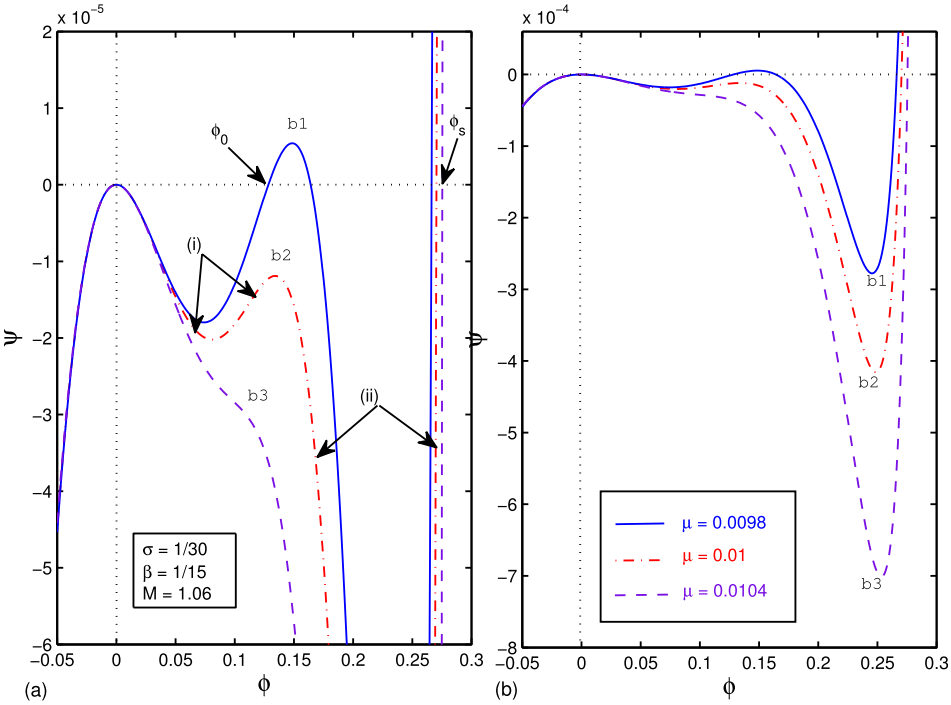

FIG. 12. Sagdeev pseudopotentials for points "$a1$" (curve "$b1$," $\mu = 0.0098$), "$a2$" (curve "$b2$," $\mu = 0.01$), and near point $a3$ (curve "$b3$," $\mu = 0.0104$) of Fig. 5, ϕ_0 (ϕ_s) being the amplitudes of the regular (super) solitary waves shown in two different scales, viz., (a) for regular, (b) for super, solitary waves, respectively.

with decreasing μ and β, it shows little or no variation in region "$B1$" ($\beta_c \le \beta \le \beta_f$), making the two sub-regions characteristically different from each other.

In Fig. 11(c) (the bottom panel), we have plotted the variation of ϕ_d, the amplitude of the compressive double layer, with β, β_d ($= 0.0648$) being the largest β value associated with a double layer solution. It shows that regions A and $B1$ of the upper two panels have no double layer solution (i.e., $PI \equiv A + B1$, $\beta_c \le \beta \le 1$), which means that, for this parameter regime, the boundary of the corresponding existence domain is solely determined by Eq. (8). On the other hand, region $B2$ (middle panel) completely coincides with PII (bottom panel, $\beta_n \le \beta \le \beta_d$), supporting both solitary waves and compressive double layers where the latter determines the upper bounds of the solitary wave solutions for this region. This reveals that the abrupt discontinuity observed in Fig. 11(b) (middle panel) as well as Fig. 5 (viz., points $a1$ and $a2$) are associated with the onset of compressive double layers. This also indicates that the two regions (viz., "PI" and "PII"), are governed by different physical processes.

Figures 12(a) and 12(b) show the Sagdeev pseudopotential curves for points "$a1$," "$a2$" and that near point "$a3$" of Fig. 5, represented as curves "$b1$" (solid line), "$b2$" (dashed-dotted), and "$b3$" (dashed line) respectively, in two different scales. In Fig. 12(a), the curve "$b1$" shows a regular solitary wave of amplitude ϕ_0 beyond which (i.e., for $\phi > \phi_0$) the pseudopotential turns positive (i.e., $\psi > 0$) making the "generalized electric field" $d\phi/d\eta$ complex, hence nonphysical. Curve "$b2$," on the other hand, shows a supersoliton[47–49] of amplitude $\approx \phi_s$ which still has two roots, like the former one, but two subwells marked by (i) and (ii), respectively. As we increase the μ value further, the subwells in curve "$b3$" tend to merge to a single one making the solution closer to a regular solitary wave, like curve "$b1$," but of substantially greater amplitude. Figure 12(b) shows the complete profiles of curves "$b1$"–"$b3$," highlighting the sharp increase in the amplitude and the depth of the pseudopotential well as it transits from "$b1$" to "$b2$." This further suggests that the latter two (viz., "$b2$" and "$b3$") belong to PI of Fig. 11, making it a different class of solution compared to that associated with "$b1$." A closer look suggests a Sagdeev pseudopotential profile between "$b1$" and "$b2$" (not shown in the figure) with three roots and two subwells[52] which marks the lower bound of solitary and supersolitary waves of PI (i.e., curves "$b2$" and "$b3$" in this case) and is associated with β_c in Fig. 11.

Previously, White *et al.*[3] reported Sagdeev pseudopotential with cusp for a three component plasma which they interpreted as large amplitude shocks. Later, Dubinov and Kolotkov[47] found Sagdeev pseudopotential profiles with two subwells for a multi-component plasma comprising of electrons, positrons, and two species of positively and negatively charged ions. They coined the name supersoliton for the said pseudopotential profile. Verheest *et al.*[48,49] showed that supersolitons may occur in a three component plasma as well. They studied the properties of supersolitons in a three component plasma in detail, emphasizing the mathematical characteristics of the corresponding pseudopotential profiles. Similar results have been confirmed by our analysis. It further confirms that supersolitons are part of a wide spectrum of solutions and are associated with a sudden change of amplitudes which resembles to a possible phase transitions of the solution as mentioned above. Recently, the existence of dust acoustic supersolitons has been confirmed in a dusty plasma.[82,83] A more detailed analysis of supersolitons is beyond the scope of the present work and will be communicated elsewhere.

E. Effects of M and σ

To complement our analysis, we have delineated the effect of M on the aforementioned parameter domains (viz.,

This article is copyrighted as indicated in the article. Reuse of AIP content is subject to the terms at: http://scitation.aip.org/termsconditions. Downloaded to IP: 14.139.123.135 On: Tue, 16 Dec 2014 06:25:22

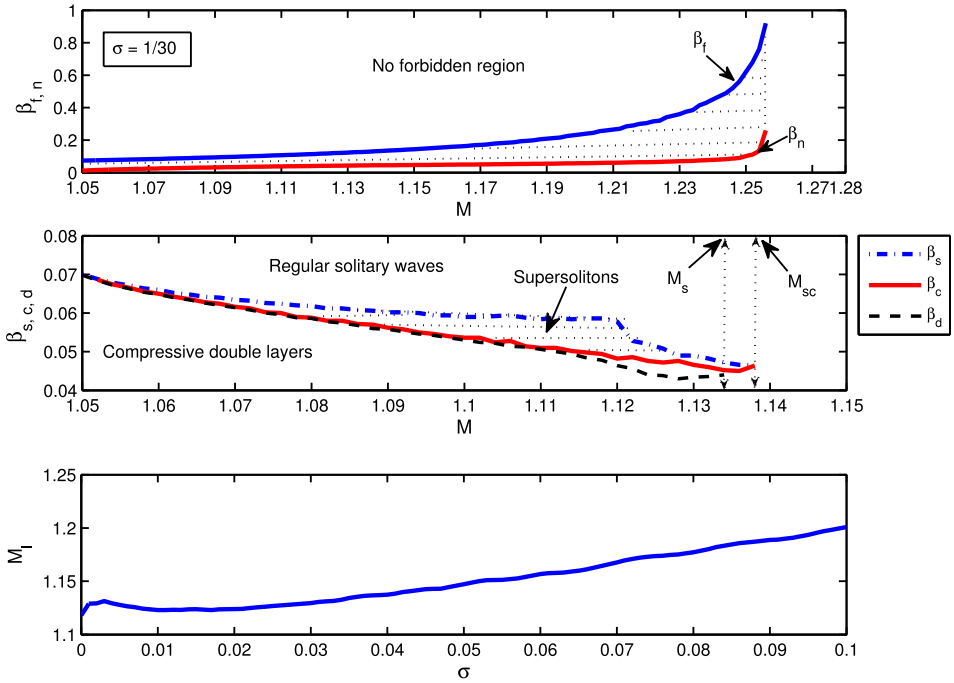

FIG. 13. Existence domains of compressive double layers and supersolitons; (a) variations of β_f and β_n with M, (b) variations of β_s, β_c and β_d with M, and (c) variations of M_l with σ.

A, B, $B1$, $B2$, etc., in Figs. 11(a)–11(c)), representing different classes of solutions. Figure 13(a) (upper panel) shows variations of β_f (solid line) and β_n (dashed-dotted) with M while the dotted area bounded between the two curves (i.e., $\beta_n \leq \beta \leq \beta_f$), represents the parameter domain where a forbidden region may occur (i.e., region B of Fig. 11). It confirms that the extent of the forbidden region increases with M (Fig. 2) while the variation of the lower bound (i.e., β_n) remains only marginal. Figure 13(b) (middle panel) shows variations of β_d (dashed line), β_c (solid line), and β_s (dashed-dotted) where β_s is the largest value of β associated with the onset of a supersoliton. The dotted area bounded between the curves β_c and β_s represents the existence domain of the supersoliton. The curves quickly merge at certain critical value of $M = M_s$ ($M = M_{sc}$) beyond which the compressive double layer (supersoliton) solutions cease to exist and only a regular solitary wave prevails. The critical values of M_s (M_{sc}) determine the respective upper boundaries of compressive double layer (supersoliton) solutions. Figure 13(c) (bottom panel) further delineates the effect of ion temperature (σ) on M_l where M_l has been determined numerically as the largest possible speed of a compressive double layer ($\approx M_d$) associated with a particular σ. Inclusion of ion temperature in a cold ion plasma have shown an initial increase, followed by a minor decrease in M_l beyond which it has increased almost linearly with σ, ensuring a faster moving compressive double layer for warmer ions.[52] The ion temperature, however, assumed to be small enough (i.e., $\sigma \leq 0.1$) to ascertain the validity of the fluid approximation.

IV. CONCLUSION

We have investigated in detail the effect of the different electron parameters, viz., β and μ, on a fully nonlinear compressive solitary wave. It has been observed that both the cold to hot electron temperature ratio (β) and the ambient density of the cooler species (μ) play a significant role to determine the amplitude and the existence domain of the solitary wave. There is a preferred value of μ ($\approx \mu_c$) which maximizes the amplitude producing a "hump" in the variation pattern and leads to a "forbidden region" in μ for a large-M solution. It further dissociates the overall existence domain into two distinct regimes. For higher values of μ, the solutions do not characteristically differ over the range of β values. "Region lh," which represents the "low β–high μ" regime, shows regular solutions with sharp increase in the amplitude with decreasing μ while the domain A in Fig. 11 is devoid of any forbidden region confirming regular solutions over all the ranges of μ. Solutions in the low-μ regime, on the other hand, significantly differ over the range of β. "Region ll," which represents the "low β–low μ" regime, confirms a delicately defined existence domain which is governed by an ultra low value of μ ($\ll 1\%$) and characterized by small amplitude solutions, anomalous width variation and compressive double layers. The region is further associated with a sudden increase in the amplitude at some critical or threshold value of β ($\approx \beta_c$) and supersolitons. A further increase in β ensures a smooth transition of supersolitons to a usual regular solitary wave. Conversely, as β decreases, it approaches to a transitional region near the threshold (i.e., $\beta \rightarrow \beta_c$, $\beta_c \leq \beta \leq \beta_s$) where a regular solitary wave solution gradually "gets deformed" to a supersoliton, followed by a sudden collapse of the amplitude. A further decrease in β beyond the threshold ($\beta < \beta_c$) leads to the aforementioned parameter domain which governs compressive double layers (e.g., $B2$ in Fig. 11).

It was further observed that the maximum speed of a compressive double layer generally increases with ion temperature, except for a very low value of σ, while an increase in the speed (M) pushes μ (or μ_x) to a vanishingly small value which may not be physically sustainable. The plasma is eventually dominated by the cooler species. The overall

This article is copyrighted as indicated in the article. Reuse of AIP content is subject to the terms at: http://scitation.aip.org/termsconditions. Downloaded to IP: 14.139.123.135 On: Tue, 16 Dec 2014 06:25:22

presence of the second species of electrons significantly modifies nonlinearity and dispersion of the system. The effect of the two electron components maximizes for $\mu \approx 15$ to 20% which coincides with the "humps" observed for the amplitude variation. Our findings are expected to be relevant for analyzing electrostatic solitary waves observed in the Earth's magnetospheric boundary layers.

ACKNOWLEDGMENTS

The authors acknowledge A. Sen, Institute for Plasma Research, Gandhinagar, India; M. A. Hellberg, University of KwaZulu-Natal, Durban, South Africa; and F. Verheest, Universiteit Gent, Gent, Belgium for stimulating discussions. Part of the work was previously supported by The Asiatic Society, Kolkata under the scheme of The Meghnad Saha Research Fellowship, and the facilities were provided by the Director and the Plasma Physics Group of Saha Institute of Nuclear Physics (SINP), Kolkata.

[1]S. S. Moiseev and R. Z. Sagdeev, J. Nucl. Energy C **5**, 43 (1963).
[2]H. Washimi and T. Taniuti, Phys. Rev. Lett. **17**, 996 (1966).
[3]R. B. White, B. D. Fried, and F. V. Coroniti, Phys. Fluids **15**, 1484 (1972).
[4]M. Q. Tran, Phys. Scr. **20**, 317 (1979).
[5]B. Buti, Astrophys. J. **268**, 420 (1983).
[6]H. Schamel and P. K. Shukla, Phys. Lett. A **192**, 71 (1994).
[7]J. F. McKenzie, F. Verheest, T. B. Doyle, and M. A. Hellberg, Phys. Plasmas **11**, 1762 (2004).
[8]M. Tribeche, R. Amour, and P. K. Shukla, Phys. Rev. E **85**, 037401 (2012).
[9]S. G. Alikhanov, V. G. Belan, and R. Z. Sagdeev, JETP Lett. **7**, 318 (1968).
[10]H. Ikeji, R. J. Taylor, and D. R. Baker, Phys. Rev. Lett. **25**, 11 (1970).
[11]Y. Nakamura, IEEE Trans. Plasma Sci. **PS-10**, 180 (1982).
[12]A. N. Sekar and Y. C. Saxena, Phys. Lett. A **105**, 233 (1984).
[13]A. Esfandyari-Kalejahi and H. Asgari, Phys. Plasmas **12**, 102302 (2005).
[14]K. B. Gylfason, J. Alami, U. Helmersson, and J. T. Gudmundsson, J. Phys. D **38**, 3417 (2005).
[15]S. K. Sharma and H. Bailung, Phys. Plasmas **17**, 032301 (2010).
[16]P. H. Sakanaka, Phys. Fluids **15**, 304 (1972).
[17]T. Sato and H. Okuda, Phys. Rev. Lett. **44**, 740 (1980).
[18]G. Chanteur, J. C. Adam, R. Pellat, and A. S. Volokhitin, Phys. Fluids **26**, 1584 (1983).
[19]C. Barnes, M. K. Hudson, and W. Lotko, Phys. Fluids **28**, 1055 (1985).
[20]V. A. Marchenko and M. K. Hudson, J. Geophys. Res. **100**, 19791, doi:10.1029/95JA01258 (1995).
[21]A. Yajima and S. Machida, Earth Planet Space **53**, 139 (2001).
[22]I. Kourakis and P. K. Shukla, J. Phys. A: Math. **36**, 11901 (2003).
[23]S. Banerjee, A. P. Mishra, P. Shukla, and L. Rondoni, Phys. Rev. E **81**, 046405 (2010).
[24]S. S. Ghosh, A. Sen, and G. S. Lakhina, Nonlinear Process. Geophys. **9**, 463 (2002).
[25]S. G. Tagare, Plasma Phys. **15**, 1247 (1973).
[26]A. K. Kalita and S. Bujarbarua, Phys. Scr. **26**, 345 (1982).
[27]A. R. Esfandyari, S. Khorram, and A. Rostami, Phys. Plasma **8**, 4753 (2001).
[28]G. C. Das and K. M. Sen, Planet Space Sci. **42**, 41 (1994).
[29]B. Sahu and R. Roychoudhury, Europhys. Lett. **100**, 15001 (2012).
[30]K. Nishinari and T. Yajima, J. Phys. Soc. Jpn. **63**, 3538 (1994).
[31]R. Böstrom, G. Gustafsson, B. Holback, G. Holmgren, H. Koshkinen, and P. Kintner, Phys. Rev. Lett. **61**, 82 (1988).
[32]S. S. Ghosh and G. S. Lakhina, Nonlinear Process. Geophys. **11**, 219 (2004).
[33]Y. Nakamura and H. Sugai, Chaos Solitons Fractals **7**, 1023 (1996).
[34]R. Z. Sagdeev, in *Reviews of Plasma Physics*, edited by M. A. Leontovich (Consultants Bureau, New York, 1966), Vol. 4, p. 23; R. Z. Sagdeev and A. A. Galeev, *Nonlinear Plasma Theory* (W. A. Benjamin, New York, 1969).
[35]S. Baboolal, R. Bharuthram, and M. A. Hellberg, J. Plasma Phys. **44**, 1 (1990).
[36]S. K. Maharaj, R. Bharuthram, S. V. Singh, and G. S. Lakhina, Phys. Plasmas **19**, 072320 (2012).
[37]S. Bujarbarua, Physica C **123**, 267 (1984).
[38]A. Luque, H. Schamel, and J.-M. Grießmeier, Phys. Plasmas **9**, 4841 (2002).
[39]H. Schamel, Phys. Plasmas **19**, 020501 (2012).
[40]B. Buti, M. Mohan, and P. K. Shukla, J. Plasma Phys. **23**, 341 (1980).
[41]R. K. Roychoudhury and S. Bhattacharyya, Can. J. Phys. **65**, 699 (1987).
[42]R. K. Roychoudhury, J. Plasma Phys. **67**, 199 (2002).
[43]S.-H. Chuang and L.-N. Hau, Phys. Plasmas **16**, 022901 (2009).
[44]S. S. Ghosh and A. N. S. Iyengar, Phys. Plasma **4**, 2139 (1997).
[45]R. Sabry, W. M. Moslem, and P. K. Shukla, Phys. Plasmas **16**, 032302 (2009).
[46]S. K. El-Labany, R. Sabry, W. F. El-Taibany, and E. A. Elghmaz, Astrophys. Space Sci. **340**, 77 (2012).
[47]A. E. Dubinov and D. Yu Kolotkov, IEEE Trans. Plasma Sci. **40**, 1429 (2012).
[48]F. Verheest, M. A. Helberg, and I. Kourakis, Phys. Plasmas **20**, 012302 (2013).
[49]F. Verheest, M. A. Hellberg, and I. Kourakis, Phys. Plasmas **20**, 082309 (2013).
[50]M. Y. Yu and H. Luo, Phys. Plasmas **15**, 024504 (2008).
[51]S. S. Ghosh, J. S. Pickett, G. S. Lakhina, J. D. Winningham, B. Lavraud, and P. M. E. Décréau, J. Geophys. Res. **113**, A06218, doi:10.1029/2007JA012768 (2008).
[52]T. K. Baluku, M. A. Helberg, and F. Verheest, Europhys. Lett. **91**, 15001 (2010).
[53]W. D. Jones, A. Lee, S. M. Gleeman, and H. J. Doucet, Phys. Rev. Lett. **35**, 1349 (1975).
[54]B. N. Goswami and B. Buti, Phys. Lett. A **57**, 149 (1976).
[55]R. Böstrom, B. Holback, and G. Holmgren, Phys. Scr. **39**, 782 (1989).
[56]S. S. Ghosh and A. N. Sekar Iyengar, Phys. Scr. **61**, 361 (2000).
[57]F. Verheest, J. Plasma Phys. **42**, 395 (1989).
[58]H. H. Matsumoto, H. Kojima, T. Miyatake, Y. Omura, M. Okada, I. Nagano, and M. Tsutsui, Geophys. Res. Lett. **21**, 2915, doi:10.1029/94GL01284 (1994).
[59]S. S. Ghosh, K. K. Ghosh, and A. N. S. Iyengar, Phys. Plasma **3**, 3939 (1996).
[60]S. S. Ghosh and A. N. Sekar Iyengar, Phys. Plasmas **4**, 3204 (1997).
[61]P. N. Murthy, S. G. Tagare, and P. S. Abrol, Can. J. Phys. **45**, 45 (1984).
[62]B. H. Quon and A. Y. Wong, Phys. Rev. Lett. **37**, 1393 (1976).
[63]H. H. Kuehl and K. Imen, IEEE Trans. Plasma Sci. **PS–13**, 37 (1985).
[64]P. C. Gray, M. K. Hudson, and W. Lotko, IEEE Trans. Plasma Sci. **PS–20**, 745 (1992).
[65]Y. Nejoh, Astrophys. Space Sci. **235**, 245 (1996).
[66]J. P. Mcfadden, C. W. Carlson, R. E. Ergun, F. S. Mozer, L. Muschietti, I. Roth, and E. Moebius, J. Geophys. Res. **108**, 8018, doi:10.1029/2002JA009485 (2003).
[67]M. K. Mishra, R. S. Tiwari, and J. K. Chawla, Phys. Plasmas **19**, 062303 (2012).
[68]R. Bharuthram and P. K. Shukla, Phys. Fluids **29**, 3214 (1986).
[69]G. S. Lakhina, B. T. Tsurutani, S. V. Singh, and R. V. Reddy, Nonlinear Process. Geophys. **10**, 65 (2003).
[70]F. Verheest and M. A. Helberg, Phys. Plasmas **17**, 102312 (2010).
[71]M. S. Alam, M. M. Masud, and A. A. Mamun, Astrophys. Space Sci. **349**, 245 (2014).
[72]K. S. Goswami and S. Bujarbarua, J. Phys. Soc. Jpn. **56**, 2396 (1987).
[73]M. K. Mishra, A. K. Arora, and R. S. Chabra, Phys. Rev. E **66**, 046402 (2002).
[74]M. K. Mishra, R. S. Tiwari, and S. K. Jain, Phys. Rev. E **76**, 036401 (2007).
[75]B. Sahu, Phys. Plasmas **18**, 082302 (2011).
[76]S. Ali Shan, A. Mushtaq, and N. Akhtar, Astrophys. Space Sci. **348**, 501 (2013).
[77]K. Ourabah and M. Tribeche, Astrophys. Space Sci. **348**, 511 (2013).
[78]S. Ghosh and R. Bharuthram, Astrophys. Space Sci. **314**, 121 (2008).
[79]F. Verheest, T. Cattaert, M. A. Helberg, and R. L. Mace, Phys. Plasmas **13**, 042301 (2006).
[80]S. S. Ghosh, Ph.D. thesis, Jadavpur University, Saha Institute of Nuclear Physics, Kolkata, 1998.
[81]F. Verheest, M. A. Helberg, N. S. Saini, and I. Kourakis, Phys. Plasmas **18**, 042309 (2011).
[82]S. K. Maharaj, R. Bharuthram, S. V. Singh, and G. S. Lakhina, Phys. Plasmas **20**, 083705 (2013).
[83]M. A. Hellberg, T. K. Baluku, F. Verheest, and I. Kourakis, J. Plasma Phys. **79**, 1039 (2013).

This article is copyrighted as indicated in the article. Reuse of AIP content is subject to the terms at: http://scitation.aip.org/termsconditions. Downloaded to IP: 14.139.123.135 On: Tue, 16 Dec 2014 06:25:22